



Boundary conditions at a gel-fluid interfaceJames J. Feng ^{1,2} and Y.-N. Young ^{3,*}¹*Department of Mathematics, University of British Columbia, Vancouver, Canada BC V6T 1Z2*²*Department of Chemical and Biological Engineering, University of British Columbia, Vancouver, Canada BC V6T 1Z3*³*Department of Mathematical Sciences, New Jersey Institute of Technology, Newark, New Jersey 07102, USA*(Received 3 August 2020; accepted 23 November 2020;
published 21 December 2020)

Hydrogels consist of a polymer skeleton hydrated by an aqueous solvent, and their hydrodynamics is often described by a coarse-grained poroelasticity model where the boundary conditions between the hydrogel and a surrounding solvent require careful consideration. Young *et al.* [*Phys. Rev. Fluids* **4**, 063601 (2019)] used the energy dissipation principle to derive a set of boundary conditions regarding the velocity jumps at the interface. However, when applied to an external shear flow over a gel layer, these conditions predict no entrained flow inside the gel, in contrast to the prediction of a previous model by Minale [*Phys. Fluids* **26**, 123102 (2014)]. We adapt the procedure of Young *et al.* to derive an alternative set of boundary conditions that does allow an external shear flow to induce shear inside the gel and compare the velocity profile to that of Minale. We also derive the limiting form of the boundary conditions in a Darcy medium.

DOI: [10.1103/PhysRevFluids.5.124304](https://doi.org/10.1103/PhysRevFluids.5.124304)**I. INTRODUCTION**

Hydrogel consists of a deformable cross-linked polymer network permeated by an aqueous solvent. As soft solids with low elastic moduli and yield stresses, hydrogels have found many applications in emerging technologies, ranging from micromechatronics to organ-on-chip devices [1,2]. The mechanics of hydrogels is dominated by the coupling between the solid skeleton and the interstitial fluid. For example, the pore space expands when fluid is injected into the gel, whereas compressing the skeleton will drive the fluid out as the pore space shrinks. This type of solid-fluid interaction can be described by poroelastic theories that treat the solid and fluid as interpenetrating continua [3,4]. Among recent studies, Cogan and Keener [5] developed a two-phase flow model for gel-like biofilms. Strychalski *et al.* [6,7] used a similar model to compute cytoplasmic flow in biological cells. MacMinn *et al.* [8] examined the coupling between the interstitial fluid flow and large deformation of a nonlinear elastic skeleton. Mori *et al.* [9] incorporated the electrochemical effect to develop a model for a polyelectrolytic gel.

As hydrogels are often employed in a liquid medium [10,11], the dynamics of the gel-fluid interface becomes an interesting question [12]. When the gel is represented by continuum-based two-phase model, the boundary conditions (BCs) between the gel and the surrounding fluid require careful analyses. This is closely associated with the long-standing problem of posing BCs between a fluid and a porous medium [13–17]. There are at least two open questions: whether there should be a discontinuity in the fluid velocity, and how the traction from the pure fluid side is partitioned into two parts to be sustained on the porous side by the interstitial fluid and the solid skeleton, respectively. The total traction from the porous side, of course, has to balance that from the pure

*Corresponding author: yyoung@njit.edu

fluid side. But without the partition, the flow in the porous medium would be underdetermined. Based on a systematic review of previous work, Minale [18–20] advocated velocity continuity and a stress partition scheme based on the void fraction.

In more recent work, Young *et al.* [21] presented an independent framework that uses the principle of energy dissipation to postulate BCs between a gel and a surrounding liquid. This led to three scalar equations linking the various velocity jumps, among the exterior pure fluid velocity \mathbf{V} , the pore fluid velocity \mathbf{v}_f , and the solid skeletal velocity \mathbf{v}_s in the gel, to the viscous tractions on the pure fluid side or the gel side or an imbalance between the two. No explicit stress partition was needed. These conditions proved highly useful as Young *et al.* [21] demonstrated small-deformation solutions of a gel sphere subject to simple shear and extensional flows of the pure fluid. Typically the normal stress imbalance on the interface acts to “inject” the surrounding fluid into the porous medium.

Curiously, when we apply the BCs of Young *et al.* [21] to a simple shear flow of the pure fluid parallel to a horizontal porous layer, a canonical one-dimensional (1D) problem considered by Minale [19], we find that the exterior shear flow cannot drive any flow in the porous medium. Specifically, the BCs of Young *et al.* [21] stipulate that the pore velocity \mathbf{v}_f (actually the velocity difference $\mathbf{v}_f - \mathbf{v}_s$, the skeletal velocity being zero in this case) be proportional to the viscous shear stress in the porous medium. This ensures that the only solution is the trivial one with no flow in the porous medium and the simple shear in the clear fluid. This contrasts the solution of Minale [19] with a sinh velocity profile in the porous medium.

To understand this contrast, we have reexamined the derivation of Young *et al.* [21], which formulates the energy-dissipation argument in terms of slip velocities $\mathbf{V} - \mathbf{v}_s$ and $\mathbf{v}_f - \mathbf{v}_s$, relative to the skeletal component of the gel. If one bases the argument instead on slip velocities relative to the pore velocity \mathbf{v}_f , different BCs result that are capable of driving a shear flow in the simple 1D shear-flow geometry. Insofar as the energy-dissipation argument suggests *sufficient but unnecessary conditions* to satisfy the second law of thermodynamics, both sets of BCs seem equally admissible.

The rest of the paper is organized as follows. In Sec. II we briefly review the two-phase flow model of Young *et al.* [21] for a gel particle in a Stokes flow and derive the set of BCs on the gel-fluid boundary. In Sec. III we demonstrate how the boundary conditions allow a exterior shear flow to drive a shear flow inside a porous medium, and compare the solution with that of Minale [19]. In Sec. IV we show that the two sets of boundary conditions reduce to nearly identical forms in the Darcy limit. We then examine the one-phase limit of the boundary conditions and discuss how the interfacial slip and permeability coefficients should vary with the volume fractions.

II. FORMULATION

A. Governing equations

We briefly summarize the two-phase flow model of Young *et al.* [21] before focusing on the BCs. Consider a drop of poroelastic gel freely suspended in a Newtonian viscous fluid (Fig. 1) with the velocity \mathbf{V} and pressure P satisfying the incompressible Stokes equations:

$$\mu \nabla^2 \mathbf{V} - \nabla P \equiv \nabla \cdot (2\mu \mathbf{E}) - \nabla P = 0, \quad (1)$$

$$\nabla \cdot \mathbf{V} = 0, \quad (2)$$

where μ is the viscosity of the exterior fluid and $\mathbf{E} \equiv [\nabla \mathbf{V} + (\nabla \mathbf{V})^T]/2$ is its strain rate tensor. The gel contains a deformable elastic skeleton fully hydrated with the same viscous fluid as the outside. The elastic skeleton and the interstitial fluid are coarse-grained into two interpenetrating continua of volume fractions ϕ_s and ϕ_f , with $\phi_f + \phi_s = 1$. The two-phase flow of this mixture obeys the following equations of motion:

$$\frac{\partial \phi_f}{\partial t} + \nabla \cdot (\phi_f \mathbf{v}_f) = 0, \quad (3)$$

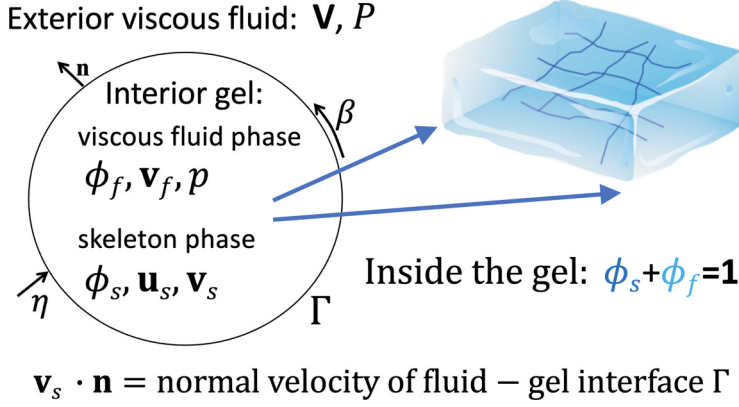


FIG. 1. A schematic of a drop of poroelastic gel in a Newtonian viscous fluid. Γ is the fluid-gel interface.

$$\frac{\partial \phi_s}{\partial t} + \nabla \cdot (\phi_s \mathbf{v}_s) = 0, \quad (4)$$

$$\nabla \cdot [\phi_f (2\mu_e \mathbf{e}_f)] - \phi_f \nabla p - \xi \phi_f \phi_s (\mathbf{v}_f - \mathbf{v}_s) = 0, \quad (5)$$

$$\nabla \cdot (\phi_s \sigma_s) - \phi_s \nabla p + \xi \phi_f \phi_s (\mathbf{v}_f - \mathbf{v}_s) = 0, \quad (6)$$

where \mathbf{v}_f is the fluid velocity, and $\mathbf{v}_s = d\mathbf{u}_s/dt$ is the skeleton velocity computed from the time derivative of the skeleton displacement \mathbf{u}_s . Note that both are “intrinsic phase averages” over a control volume that contains only the fluid or solid material [18]. $\mathbf{e}_f \equiv [\nabla \mathbf{v}_f + (\nabla \mathbf{v}_f)^T]/2$, and μ_e is the effective viscosity of the fluid phase. Two commonly used assumptions are $\mu_e = \mu$ [21,22] and $\mu_e = \mu/\phi_f$ [16,19,23]. We will adopt the latter, although this choice does not affect the narrative of this paper. The same pressure p is shared by both phases. ξ is a constant friction coefficient between the two phases; it can be related to the permeability K in the usual form of the Brinkman equation as $\xi = \mu/(\phi_s K)$. Finally, σ_s is the solid stress tensor that, assuming linear elasticity for simplicity, can be related to the strain tensor $\varepsilon \equiv [\nabla \mathbf{u}_s + (\nabla \mathbf{u}_s)^T]/2$ by

$$\sigma_s = \Lambda \text{tr}(\varepsilon) \mathbf{I} + (\mathcal{M} - \Lambda) \varepsilon, \quad (7)$$

with \mathcal{M} being the p -wave modulus and Λ Lamé’s first parameter. We have taken the skeleton to be purely elastic and ignored any viscous component in its mechanical response.

B. Boundary conditions

To pose BCs on the interface between the gel particle and the exterior fluid, we first note three conditions dictated by the kinematics, continuity of fluid flow, and traction balance across the interface Γ :

$$\mathbf{n} \cdot \mathbf{v}_s = v_\Gamma, \quad (8)$$

$$\mathbf{n} \cdot (\mathbf{V} - \mathbf{v}_s) = \phi_f \mathbf{n} \cdot (\mathbf{v}_f - \mathbf{v}_s), \quad (9)$$

$$\mathbf{n} \cdot (2\mu \mathbf{E} - p \mathbf{I}) = \mathbf{n} \cdot [\phi_s \sigma_s + \phi_f (2\mu_e \mathbf{e}_f) - p \mathbf{I}], \quad (10)$$

where \mathbf{n} is the outward unit normal vector on the gel surface, and v_Γ is the normal velocity of the interface. These are the same as in Young *et al.* [21]. Note that we have neglected the gel-fluid interfacial tension in the traction balance.

To derive the additional BCs regarding the velocity jumps on the interface, Mori *et al.* [9] and Young *et al.* [21] examined the energy dissipation of the whole system and posed BCs to ensure that the interface dissipates energy from the system. Such an argument is rooted in the second law of thermodynamics [24]. However, we stress that the argument gives a sufficient condition and does not guarantee a unique set of boundary conditions. Following Young *et al.* [21], we multiply Eqs. (1), (5), and (6) by \mathbf{V} , \mathbf{v}_f , and \mathbf{v}_s , respectively, and sum up the three products. Then the requirement that the free energy of the system decrease in time amounts to requiring that the following surface integral be nonpositive:

$$I_\Gamma = \int_\Gamma \{-\mathbf{V} \cdot (2\mu\mathbf{E} - P\mathbf{I}) + \mathbf{v}_f \cdot [\phi_f(2\mu_e\mathbf{e}_f) - \phi_f p\mathbf{I}] + \mathbf{v}_s \cdot (\phi_s\sigma_s - \phi_s p\mathbf{I})\} \cdot \mathbf{n} ds \leq 0. \quad (11)$$

The minus sign in front of \mathbf{V} is because \mathbf{n} is the *inward* normal vector to the pure-fluid domain. Defining velocity jumps $\tilde{\mathbf{V}} \equiv \mathbf{V} - \mathbf{v}_s$ and $\tilde{\mathbf{v}}_f \equiv \mathbf{v}_f - \mathbf{v}_s$ with respect to the solid velocity \mathbf{v}_s , Young *et al.* [21] showed that one way to satisfy the above is to pose the following BCs for the velocity jumps at the interface (called BC1 hereafter for brevity):

$$(\mathbf{V} - \mathbf{v}_s) \cdot \mathbf{n} = \eta \mathbf{n} \cdot [(2\mu\mathbf{E} - P\mathbf{I}) - (2\mu_e\mathbf{e}_f - p\mathbf{I})] \cdot \mathbf{n}, \quad (12)$$

$$(\mathbf{V} - \mathbf{v}_s) \cdot \mathbf{t} = \beta \mathbf{n} \cdot (2\mu\mathbf{E}) \cdot \mathbf{t}, \quad (13)$$

$$\phi_f(\mathbf{v}_f - \mathbf{v}_s) \cdot \mathbf{t} = -\beta \mathbf{n} \cdot (2\mu_e\mathbf{e}_f) \cdot \mathbf{t}, \quad (14)$$

where $\eta > 0$ is an interfacial permeability and $\beta > 0$ is an interfacial slip coefficient. We have inserted the factor of 2 on the right-hand sides of Eqs. (13) and (14) to be consistent with the form of the viscous stress tensors. This slight alteration from the original notation of Young *et al.* [21] does not affect the essence of the BCs. As shown in Sec. III, this set of BCs does not allow a simple shear flow V to drive any flow \mathbf{v}_f in a porous medium.

To derive an alternative set of BCs, we deviate from Young *et al.* [21] by introducing relative velocities not with respect to \mathbf{v}_s but with respect to \mathbf{v}_f :

$$\tilde{\tilde{\mathbf{V}}} \equiv \mathbf{V} - \mathbf{v}_f, \quad \tilde{\tilde{\mathbf{v}}}_s \equiv \phi_s(\mathbf{v}_s - \mathbf{v}_f).$$

It is easy to see that $\tilde{\tilde{\mathbf{V}}} - \tilde{\tilde{\mathbf{v}}}_s = \mathbf{V} - (\phi_f\mathbf{v}_f + \phi_s\mathbf{v}_s) = \mathbf{V} - \mathbf{q}$ is the ‘‘slip velocity’’ between the pure fluid and the composite velocity of the porous medium, and that $(\tilde{\tilde{\mathbf{V}}} - \tilde{\tilde{\mathbf{v}}}_s) \cdot \mathbf{n} = 0$ according to Eq. (9). Both properties are the same as possessed by $\tilde{\mathbf{V}}$ and $\tilde{\mathbf{v}}_f$ in the original derivation of Young *et al.* [21]. Now we focus on the two tilde jump velocities.

Using the tilde velocities, we rewrite the surface integrals as

$$\begin{aligned} I_\Gamma &= \int_\Gamma -\tilde{\mathbf{V}} \cdot (2\mu\mathbf{E} - P\mathbf{I}) \cdot \mathbf{n} ds + \int_\Gamma \tilde{\mathbf{v}}_s \cdot [\sigma_s - p\mathbf{I}] \cdot \mathbf{n} ds \\ &\quad + \int_\Gamma \mathbf{v}_f \cdot [\phi_f(2\mu_e\mathbf{e}_f) - \phi_f p\mathbf{I} + \phi_s\sigma_s - \phi_s p\mathbf{I} - 2\mu\mathbf{E} + P\mathbf{I}] \cdot \mathbf{n} ds \\ &= \int_\Gamma -\tilde{\mathbf{V}} \cdot (2\mu\mathbf{E} - P\mathbf{I}) \cdot \mathbf{n} ds + \int_\Gamma \tilde{\mathbf{v}}_s \cdot [\sigma_s - p\mathbf{I}] \cdot \mathbf{n} ds, \end{aligned} \quad (15)$$

where the second line vanishes for the overall traction balance on the interface (10) as in Young *et al.* [21]. Decomposing the tilde velocities into normal and tangential components (e.g., $\tilde{\mathbf{V}}_\perp = \tilde{\mathbf{V}} \cdot \mathbf{nn}$, $\tilde{\mathbf{V}}_\parallel = \tilde{\mathbf{V}} \cdot \mathbf{tt}$), and noting $\tilde{\tilde{\mathbf{V}}}_\perp = \tilde{\tilde{\mathbf{v}}}_{s\perp}$, we have

$$\begin{aligned} I_\Gamma &= - \int_\Gamma \tilde{\mathbf{V}}_\perp \cdot (2\mu\mathbf{E} - P\mathbf{I} - \sigma_s + p\mathbf{I}) \cdot \mathbf{n} ds - \int_\Gamma \tilde{\mathbf{V}}_\parallel \cdot (2\mu\mathbf{E} - P\mathbf{I}) \cdot \mathbf{n} ds \\ &\quad + \int_\Gamma \tilde{\tilde{\mathbf{v}}}_{s\parallel} \cdot (\sigma_s - p\mathbf{I}) \cdot \mathbf{n} ds. \end{aligned} \quad (16)$$

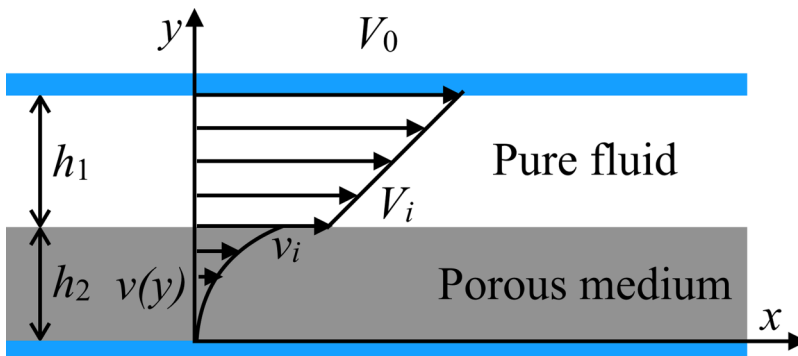


FIG. 2. A schematic showing the shear-flow geometry considered by Minale [19]. A layer of gel lies atop a rigid substrate, and a viscous fluid undergoes a simple shear above the gel parallel to the gel-fluid interface.

Similar to Young *et al.* [21], we postulate the following linear relationships to ensure positive energy dissipation (called BC2 hereafter):

$$\tilde{\mathbf{V}}_{\perp} \equiv (\mathbf{V} - \mathbf{v}_f) \cdot \mathbf{nn} = \tilde{\eta} [\mathbf{n} \cdot (2\mu\mathbf{E} - P\mathbf{I} - \sigma_s + p\mathbf{I}) \cdot \mathbf{n}] \mathbf{n}, \quad (17)$$

$$\tilde{\mathbf{V}}_{\parallel} \equiv (\mathbf{V} - \mathbf{v}_f) \cdot \mathbf{tt} = \tilde{\beta} [\mathbf{n} \cdot (2\mu\mathbf{E}) \cdot \mathbf{t}] \mathbf{t}, \quad (18)$$

$$\tilde{\mathbf{v}}_{s\parallel} \equiv \phi_s(\mathbf{v}_s - \mathbf{v}_f) \cdot \mathbf{tt} = -\tilde{\beta} (\mathbf{n} \cdot \sigma_s \cdot \mathbf{t}) \mathbf{t}, \quad (19)$$

with positive constants $\tilde{\eta} > 0$ and $\tilde{\beta} > 0$. These BCs look similar to that of the original BCs of Young *et al.* [21] [Eqs. (12)–(14)], but with some distinct features:

(i) The normal velocity difference is $\tilde{\mathbf{V}}_{\perp} = \tilde{\mathbf{v}}_{s\perp} = \phi_s(\mathbf{v}_s - \mathbf{v}_f) \cdot \mathbf{nn}$. Thus, Eq. (17) implies that the normal stress imbalance between the outer fluid and the *solid skeleton* injects the pore fluid into the gel. In Eq. (12) the pore fluid is injected by the imbalance between the normal stresses of the *fluids* on both sides of the boundary. Note the convention that the normal stress is negative when compressive.

(ii) Equation (18) implies that the viscous shear stress of the outer fluid drives the tangential slip velocity between the outer fluid and the pore fluid, as opposed to the slip velocity between the outer fluid and the solid skeleton in Eq. (13).

(iii) Equation (19) gives us the slip velocity between the fluid and solid components on the gel side of the interface and can be rewritten as

$$(\mathbf{v}_f - \mathbf{v}_s) \cdot \mathbf{t} = \frac{\tilde{\beta}}{\phi_s} (\mathbf{n} \cdot \sigma_s \cdot \mathbf{t}) = \frac{\tilde{\beta}}{\phi_s^2} \mathbf{n} \cdot (2\mu\mathbf{E} - \phi_f 2\mu_e \mathbf{e}_f) \cdot \mathbf{t} \quad (20)$$

by virtue of the overall balance in tangential stresses across the interface (10). The right-hand-side of Eq. (20) consists in the imbalance in the viscous shear stress between the fluids on either side of the interface. This imbalance may drive a tangential flow of the pore fluid if we apply the BC to the 1D shear-flow geometry of Minale [19] (Fig. 2). This contrasts the original boundary condition of Young *et al.* [21] (14), where the tangential flow is driven by the viscous shear stress in the pore fluid alone.

The two derivations differ only in the definition of the velocity jumps (relative to the skeletal velocity \mathbf{v}_s or the interstitial fluid velocity \mathbf{v}_f). Yet the resulting BC1 and BC2 have materially different implications for the flow field in the gel. Both differ from the BCs of Minale [19]. They obviate the need for partitioning the total traction from the exterior fluid into two parts to be sustained by the skeleton and the interstitial fluid on the gel side. Besides, Minale [19] has asserted $\mathbf{V} = \mathbf{q}$ as a boundary condition [his Eq. (51)]. In BC1 and BC2, the normal component of $\mathbf{V} - \mathbf{q} = \mathbf{V} - \phi_f \mathbf{v}_f - \phi_s \mathbf{v}_s$ vanishes because of mass conservation of the fluid. Its tangential

TABLE I. The two complete sets of boundary conditions.

Physical meaning	BC1	BC2
Kinematics	$\mathbf{n} \cdot \mathbf{v}_s = v_\Gamma$	
Fluid continuity	$\mathbf{n} \cdot (\mathbf{V} - \mathbf{v}_s) = \phi_f \mathbf{n} \cdot (\mathbf{v}_f - \mathbf{v}_s)$	
Total traction balance	$\mathbf{n} \cdot (2\mu\mathbf{E} - p\mathbf{I}) = \mathbf{n} \cdot [\phi_s \sigma_s + \phi_f (2\mu_e \mathbf{e}_f) - p\mathbf{I}]$	
Normal velocity jump	$(\mathbf{V} - \mathbf{v}_s) \cdot \mathbf{n} = \eta \mathbf{n} \cdot [(2\mu\mathbf{E} - p\mathbf{I}) - (2\mu_e \mathbf{e}_f - p\mathbf{I})] \cdot \mathbf{n}$	$(\mathbf{V} - \mathbf{v}_f) \cdot \mathbf{n} = \eta \mathbf{n} \cdot [(2\mu\mathbf{E} - p\mathbf{I}) - (\sigma_s - p\mathbf{I})] \cdot \mathbf{n}$
Tangential velocity jump	$(\mathbf{V} - \mathbf{v}_s) \cdot \mathbf{t} = \beta \mathbf{n} \cdot (2\mu\mathbf{E}) \cdot \mathbf{t}$	$(\mathbf{V} - \mathbf{v}_f) \cdot \mathbf{t} = \beta \mathbf{n} \cdot (2\mu\mathbf{E}) \cdot \mathbf{t}$
Interphasic velocity jump	$\phi_f (\mathbf{v}_f - \mathbf{v}_s) \cdot \mathbf{t} = -\beta \mathbf{n} \cdot (2\mu_e \mathbf{e}_f) \cdot \mathbf{t}$	$\phi_s (\mathbf{v}_s - \mathbf{v}_f) \cdot \mathbf{t} = -\beta \mathbf{n} \cdot \sigma_s \cdot \mathbf{t}$

component can be computed by subtracting Eq. (14) from (13) or subtracting Eq. (19) from (18):

$$(\mathbf{V} - \mathbf{q}) \cdot \mathbf{t} = \begin{cases} \beta \mathbf{n} \cdot (2\mu\mathbf{E} + 2\mu_e \mathbf{e}_f) \cdot \mathbf{t} & \text{(BC1)} \\ \beta \mathbf{n} \cdot (2\mu\mathbf{E} + \sigma_s) \cdot \mathbf{t} & \text{(BC2)} \end{cases}. \quad (21)$$

Both slip velocities are similar to that derived by Angot *et al.* [25] via a boundary layer asymptotic analysis. Their tangential velocity jump is proportional to the mean of the tangential stresses on both sides of the interface [Eq. (40) therein].

For later reference, we summarize the two sets of boundary conditions in Table I.

III. 1D SHEAR FLOW DRIVEN BY AN EXTERIOR FLOW

When a viscous fluid flows over a poroelastic gel layer (Fig. 2), one may expect an entrained flow inside the porous medium. Such is the prediction of the BCs due to Minale [19]. Using BC1 of Young *et al.* [21], one can show that the steady solution has zero flow inside the porous medium ($\mathbf{v}_f = \mathbf{v}_s = 0$) and a tangential slip $V_i = \beta\mu(dV/dy)$ above the interface ($y = h_2^+$). We will show that BC2 allows a tangential flow to be driven inside the gel, and the 1D steady-state solution will have a linear velocity profile in the pure fluid and a sinh profile $v(y)$ inside the gel, with tangential velocities V_i and v_i on either side of the interface. The solid skeleton sustains a shear stress and deforms to a finite strain, with $\mathbf{v}_s = 0$ everywhere.

The slip velocity $V_i - v_i$ can be calculated from Eq. (18):

$$V_i - v_i = \beta\mu \frac{V_0 - V_i}{h_1}. \quad (22)$$

Then Eq. (20) gives v_i in terms of the viscous shear stress mismatch across the interface, after assuming $\mu_e = \mu/\phi_f$:

$$v_i = \frac{\beta\mu}{(1 - \phi_f)^2} \left(\frac{V_0 - V_i}{h_1} - \left. \frac{dv}{dy} \right|_{y=h_2} \right). \quad (23)$$

The flow inside the gel of permeability K is governed by the Brinkman equation with zero pressure gradient:

$$\frac{d^2 v}{dy^2} = \frac{\phi_f}{K} v, \quad (24)$$

whose solution gives the following velocity profile inside the gel after applying the no-slip BC on the substrate $v(0) = 0$:

$$v(y) = C \sinh \left(y \sqrt{\frac{\phi_f}{K}} \right). \quad (25)$$

Although the Brinkman equation typically implies a “phase-averaged” velocity [19], which corresponds to our v/ϕ_f , the distinction is subsumed into the constant C . Substituting v and its gradient at $y = h_2$ into Eqs. (22) and (23) leads to two linear equations for the constants V_i and C :

$$V_i - C \sinh \left(h_2 \sqrt{\frac{\phi_f}{K}} \right) = \frac{\beta\mu}{h_1} (V_0 - V_i), \quad (26)$$

$$C \sinh \left(h_2 \sqrt{\frac{\phi_f}{K}} \right) = \frac{\beta\mu}{h_1(1-\phi_f)^2} \left[V_0 - V_i - C h_1 \sqrt{\frac{\phi_f}{K}} \cosh \left(h_2 \sqrt{\frac{\phi_f}{K}} \right) \right]. \quad (27)$$

Introducing dimensionless parameters and shorthand notations: $\phi = \phi_f$ (constant porosity or void fraction), $\alpha = \beta\mu/h_1$ (ratio of slip length to macroscopic length), $\gamma = h_1\sqrt{\phi/K}$ (ratio of macroscopic length to pore size), $s = \sinh(h_2\sqrt{\phi/K})$, and $c = \cosh(h_2\sqrt{\phi/K})$, we write the solution in dimensionless form for the two scaled unknowns V_i/V_0 and C/V_0 :

$$\frac{V_i}{V_0} = \alpha \frac{c\alpha\gamma + s(2 - 2\phi + \phi^2)}{c\alpha(1 + \alpha)\gamma + s[\alpha + (1 + \alpha)(1 - \phi)^2]}, \quad (28)$$

$$\frac{C}{V_0} = \frac{\alpha}{c\alpha(1 + \alpha)\gamma + s[\alpha + (1 + \alpha)(1 - \phi)^2]}. \quad (29)$$

Now the interstitial fluid velocity in the gel is

$$\frac{v(y)}{V_0} = \frac{\alpha}{c\alpha(1 + \alpha)\gamma + s[\alpha + (1 + \alpha)(1 - \phi)^2]} \sinh \left(y \sqrt{\frac{\phi}{K}} \right), \quad (30)$$

with the interfacial velocity $v_i = v(h_2) = Cs$.

We have few data on fluid flow perfusing a hydrogel and it is not straightforward to estimate the permeability K . For other types of porous media, sizable data exist in the literature, and Nishiyama and Yokoyama [26] suggested $K = 0.01\phi a^2$ for sandstones, where ϕ is the porosity and a is the averaged pore radius. The typical pore sizes in mucin and other polymer gels range from 100 nm to 500 nm [27–30]. The porosity of hydrogels varies according to the degree of hydration, from 0.5 to 0.93 [31–33]. Taking medium values of $\phi = 0.8$ and $a = 100$ nm, we can estimate $K = 8 \times 10^{-5} \mu\text{m}^2$. If we take the layer thicknesses to be $h_1 = h_2 = 0.5$ mm for a typical microfluidic device, the layer-to-pore size ratio $\gamma = h_1\sqrt{\phi/K} = 5 \times 10^4$ is very large and $s/c = \tanh(h_2\sqrt{\phi/K}) \approx 1$. For the slip length $b = \beta\mu$, typical estimations fall in the range of 1–100 nm [34]. Then the ratio $\alpha = \beta\mu/h_1 = 2 \times 10^{-6}$ to 2×10^{-4} is very small. In this case $v_i/V_0 \sim \alpha \ll 1$ and there is hardly any flow in the gel layer, as can be intuitively anticipated. The gel layer is essentially impermeable: $V_i \approx 0$, $v_i \approx 0$, $v(y) \approx 0$. This is approximately the same solution as produced by BC1 of Young *et al.* [21]

If we consider a porous gel with very large pores ($\gamma = 25$) and large interfacial slip, and the same $\phi = 0.8$, we can plot the dimensionless interfacial velocities V_i/V_0 and v_i/V_0 , as well as the slip velocity $(V_i - v_i)/V_0$ as functions of the dimensionless slip length α (Fig. 3). Whereas V_i increases monotonically with α , differentiating Eq. (29) confirms that v_i reaches a maximum at $\alpha = (1 - \phi)\sqrt{s/(c\gamma)} \approx 0.04$ for the current parameters. This can be rationalized as follows. As v_i initially rises with α , so does the Brinkman shear stress on the gel side. Meanwhile, a rising V_i reduces the shear rate and shear stress in the pure fluid. Thus, the jump in shear stress across the interface decreases with α in Eq. (23), and this eventually leads to a decline in v_i .

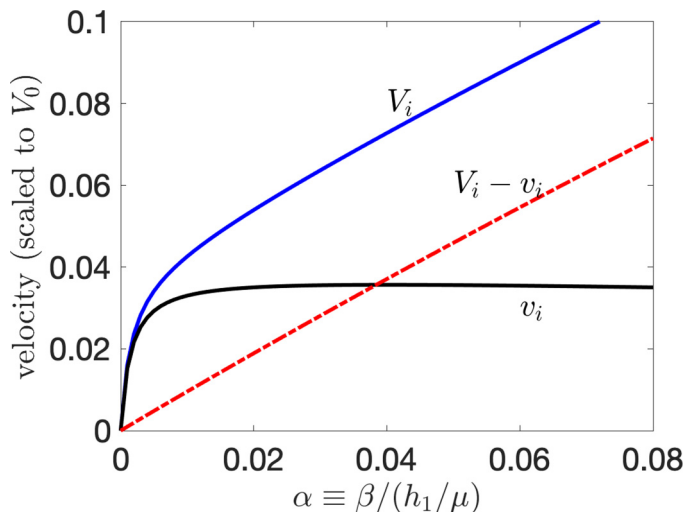


FIG. 3. For a gel with porosity $\phi = 0.8$ and a large pore size ($\gamma = 25$), the model predicts an interfacial velocity V_i on the pure-fluid side that increases with the slip ratio α . Interestingly, the interfacial velocity v_i on the gel side exhibits a maximum at $\alpha \approx 0.04$. The interfacial slip $V_i - v_i$ also increases with α .

For $\alpha = 0.01$, the fluid velocity profile is plotted in Fig. 4 as a function of the dimensionless coordinate $y\sqrt{\phi/K}$ (solid black curves). It comprises two segments: the interstitial fluid velocity $v(y)/V_0$ inside the gel layer ($y\sqrt{\phi/K} < \gamma = 25$) and the pure fluid velocity $V(y)/V_0$ above it. The inset shows a magnified view of the interfacial region. Notice first the discontinuity in the tangential velocity across the interface; Eq. (22) requires a faster flow on the pure-fluid side than on the gel side of the interface. Moreover, the shear rate is also greater on the pure-fluid side due to Eq. (23).

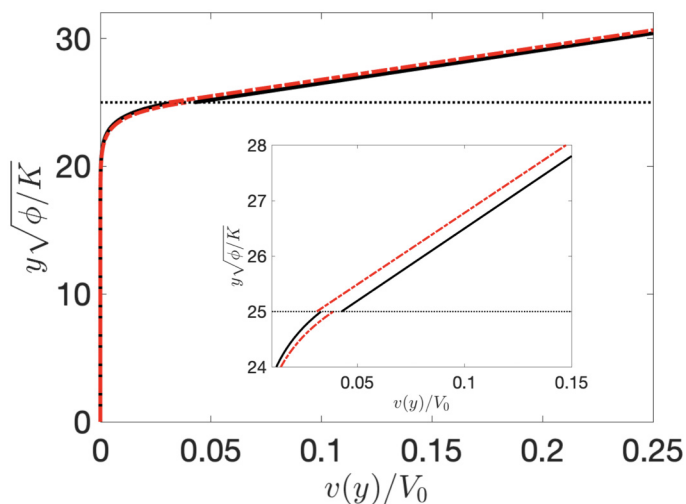


FIG. 4. Velocity profile in the 1D shear-flow solution for a gel layer with large pores ($\gamma = 25$), large slip ($\alpha = 0.01$) and moderate porosity $\phi = 0.8$. The y axis is the dimensionless coordinate $y\sqrt{\phi/K}$, with the interface at $y\sqrt{\phi/K} = \gamma = 25$ (dotted horizontal line). On the pure-fluid side, only a small portion of the linear profile is plotted. The solid curves are the velocity profile for BC2 in this work, and the dash-dotted curves are prediction of Minale's model.

The velocity profile can be compared with what the Minale model [19] predicts for the same parameters. While we have used “intrinsic-phase-averaged” quantities exclusively, Minale [19] used them alongside “phase-averaged” ones. Converting to our notations and again taking $\mu_e = \mu/\phi_f$, we can reduce his boundary conditions [Eqs. (51) and (56) in Minale [19]] to

$$\phi v_i = V_i, \quad (31)$$

$$\left. \frac{dv}{dy} \right|_{h_2} = \left. \frac{dV}{dy} \right|_{h_2}. \quad (32)$$

With the general solution for the velocity profile $v(y) = C \sinh(y\sqrt{\phi/K})$, these BCs lead to the following solution:

$$\frac{C}{V_0} = \frac{1}{c\gamma + s\phi}, \quad \frac{v_i}{V_0} = \frac{s}{c\gamma + s\phi}, \quad \frac{V_i}{V_0} = \frac{s\phi}{c\gamma + s\phi}, \quad \frac{v(y)}{V_0} = \frac{1}{c\gamma + s\phi} \sinh\left(y\sqrt{\frac{\phi}{K}}\right). \quad (33)$$

The velocity profile (red dash-dotted curves) is compared with ours in Fig. 4.

Note first that the interfacial velocities v_i and V_i of Eq. (33) are constants, independent of a slip coefficient, as none exists in Minale’s model. The Minale v_i is always slightly above ours for any slip length; our v_i peaks around $\alpha = 0.04$, and that is when the two profiles are the closest. Second, Eq. (31) implies $v_i > V_i$, namely, a greater pore fluid velocity on the gel side than the velocity on the pure-fluid side. This is opposite the jump predicted by our BC2, as illustrated in Fig. 4. Finally, Eq. (32) comes from a stress partition that, interestingly, requires equal shear rates across the interface in our notation. In our model, this would imply a larger Brinkman shear stress on the gel side than the constant stress in the pure fluid. This difference stems from a slight discrepancy in the momentum equations between the two models. For example, for the 1D shear flow of Fig. 2, the shear-stress balance across the interface amounts to $\phi_s \sigma_s + \phi_f^2 \mu_f (dv/dy) = \mu (dV/dy)$ in Minale’s model, whereas our model [Eq. (10)] has ϕ_f instead of ϕ_f^2 in the second term.

IV. LIMITING CASES

A. The Darcy limit

When the viscous dissipation in the gel is dominated by the interphasic friction, the Brinkman stress can be neglected to reduce the Brinkman equation to Darcy’s law. The vanishing of $\nabla^2 \mathbf{v}_f$ means that fewer BCs are needed, and thus it is interesting to examine the limiting form of the two sets of BCs. Note that even when a system of differential equations reduces to a limiting form, its solution does not necessarily approach that of the reduced system. This has been demonstrated recently in the Stokes limit of the Brinkman flow ($\xi \rightarrow 0$) [35]. Here we do not concern ourselves with the limiting behavior of the solutions.

First, the total traction balance (10) reduces to

$$\mathbf{n} \cdot (2\mu\mathbf{E} - P\mathbf{I}) = \mathbf{n} \cdot (\phi_s \sigma_s - p\mathbf{I}). \quad (34)$$

Of the three velocity jumps in BC1 [Eqs. (12)–(14)], the interphasic slip condition (14) should be omitted in the Darcy limit. The reason is that this condition stems from the viscous dissipation of the Brinkman term. Now that this term vanishes from the momentum equation (5) and the surface integral for energy dissipation (11), Eq. (14) would not have been postulated to begin with. Thus, BC1 reduces to the following two conditions:

$$(\mathbf{V} - \mathbf{v}_s) \cdot \mathbf{n} = \eta \mathbf{n} \cdot (2\mu\mathbf{E} - P\mathbf{I} + p\mathbf{I}) \cdot \mathbf{n} = \eta \phi_s \mathbf{n} \cdot \sigma_s \cdot \mathbf{n}, \quad (35)$$

$$(\mathbf{V} - \mathbf{v}_s) \cdot \mathbf{t} = \beta \mathbf{n} \cdot (2\mu\mathbf{E}) \cdot \mathbf{t} = \beta \phi_s \mathbf{n} \cdot \sigma_s \cdot \mathbf{t}, \quad (36)$$

where the exterior viscous stresses can be replaced by the solid stresses by using the traction balance of Eq. (34).

The Darcy limit of BC2 is not as straightforward. The adoption of relative velocities with respect to \mathbf{v}_f still leads to the three dyads in the surface energy dissipation of Eq. (16), none of which drops out by virtue of a vanishing Brinkman stress. Using the traction balance of Eq. (34), we can rewrite Eq. (16) as

$$\begin{aligned} I_\Gamma &= \int_\Gamma \tilde{\mathbf{V}}_\perp \cdot \phi_f \sigma_s \cdot \mathbf{n} ds - \int_\Gamma \tilde{\mathbf{V}}_\parallel \cdot (2\mu\mathbf{E}) \cdot \mathbf{n} ds + \int_\Gamma \tilde{\mathbf{v}}_{s\parallel} \cdot (2\phi_s^{-1}\mu\mathbf{E}) \cdot \mathbf{n} ds \\ &= \int_\Gamma \tilde{\mathbf{V}}_\perp \cdot \phi_f \sigma_s \cdot \mathbf{n} ds - \int_\Gamma (\tilde{\mathbf{V}}_\parallel - \phi_s^{-1}\tilde{\mathbf{v}}_{s\parallel}) \cdot (2\mu\mathbf{E}) \cdot \mathbf{n} ds \\ &= \int_\Gamma (\mathbf{V} - \mathbf{v}_f) \cdot \mathbf{n} (\phi_f \mathbf{n} \cdot \sigma_s \cdot \mathbf{n}) ds - \int_\Gamma (\mathbf{V} - \mathbf{v}_s) \cdot \mathbf{t} [\mathbf{n} \cdot (2\mu\mathbf{E}) \cdot \mathbf{t}] ds. \end{aligned}$$

To ensure its nonpositiveness, we postulate the following two conditions as the Darcy limit of BC2:

$$(\mathbf{V} - \mathbf{v}_f) \cdot \mathbf{n} = -\eta \phi_f \mathbf{n} \cdot \sigma_s \cdot \mathbf{n}, \quad (37)$$

$$(\mathbf{V} - \mathbf{v}_s) \cdot \mathbf{t} = \beta \mathbf{n} \cdot 2\mu\mathbf{E} \cdot \mathbf{t}. \quad (38)$$

In view of the traction balance of Eq. (34), it is easy to see that Eq. (37) is the same as Eq. (17) of the original BC2. Equation (38) can be recovered by taking the difference between Eq. (18) and Eq. (19)/ ϕ_s , and then redefining the slip coefficient $\beta \equiv \tilde{\beta}(1 + 1/\phi_s^2)$.

Note the similarity between BC1 and BC2 in the Darcy limit. Both relate the velocity jumps to the normal and shear stress of the solid stress tensor σ_s , the shear stress being equal to that of the exterior flow owing to Eq. (34). In particular, the ‘‘Navier slip condition’’ is identical between Eqs. (36) and (38). The ‘‘permeability conditions,’’ i.e., the normal velocity jumps of Eqs. (35) and (37), seem to differ more significantly. But a connection can be made in the special case of *steady-state* flows in a Darcy medium. The steady-state shape of the interface and the continuity of fluid flow imply

$$\mathbf{v}_s \cdot \mathbf{n} = 0, \quad \mathbf{V} \cdot \mathbf{n} = \phi_f \mathbf{v}_f \cdot \mathbf{n}.$$

Then Eqs. (35) and (37) become essentially the same, subject to a differing η value.

This common limit in steady Darcy flows is intriguing for two reasons. First, BC1 and BC2 will predict essentially the same equilibrium deformation of a Darcy drop under a steady extensional or shear flow. Such steady solutions, as obtained analytically by Young *et al.* [21] in the small-deformation limit, will not be a revealing test on the relative merit of BC1 and BC2. For that purpose, therefore, one will need to compare solutions of nontrivial Brinkman flows or unsteady transients, which are probably accessible only by numerical computation. Second, reconsider the disparate predictions of BC1 and BC2 for the 1D shear problem of Sec. III. BC1 predicts zero flow inside the gel while BC2 predicts a shear flow profile $v(y)$ that varies in space, thereby inducing a Brinkman stress. Now if one insists on a *uniform Darcy flow* inside the porous medium, naturally an external shear flow will not be able to drive such a flow into arbitrary depth of the porous medium. Thus, the predictions of BC2 converges to that of BC1 in the Darcy limit as expected.

B. The one-phase limits

In deriving BC1 and BC2, the positivity of interfacial dissipation requires only the interfacial slip coefficient β and the interfacial permeability η to be positive. They are not required to be constants. In fact, Young *et al.* [21] provided a scaling argument that required $\beta \rightarrow 0$ as $\phi_s \rightarrow 0$. In this section we consider the limits of $\phi_f \rightarrow 0$ (the porous medium turning into impermeable elastic solid) and $\phi_f \rightarrow 1$ (the porous medium turning into pure liquid) to ensure that our boundary conditions are physically consistent in these limits.

In the limit of $\phi_f \rightarrow 0$, the boundary conditions of Table I reduce to those in Table II, where the total traction balance has been used to simplify the normal velocity jump conditions. To approach the no-penetration and no-slip conditions on a fluid-solid interface, BC1 requires $\beta \rightarrow 0$ and $\eta \rightarrow 0$

BOUNDARY CONDITIONS AT A GEL-FLUID INTERFACE

 TABLE II. The two sets of boundary conditions in the limit of $\phi_f \rightarrow 0$.

Physical meaning	BC1	BC2
Kinematics	$\mathbf{n} \cdot \mathbf{v}_s = v_\Gamma$	
Fluid continuity	$\mathbf{n} \cdot (\mathbf{V} - \mathbf{v}_s) = 0$	
Total traction balance	$\mathbf{n} \cdot (2\mu\mathbf{E} - P\mathbf{I}) = \mathbf{n} \cdot (\sigma_s - p\mathbf{I})$	
Normal velocity jump	$(\mathbf{V} - \mathbf{v}_s) \cdot \mathbf{n} = \eta \mathbf{n} \cdot (\sigma_s - 2\mu_e \mathbf{e}_f) \cdot \mathbf{n}$	$(\mathbf{V} - \mathbf{v}_f) \cdot \mathbf{n} = 0$
Tangential velocity jump	$(\mathbf{V} - \mathbf{v}_s) \cdot \mathbf{t} = \beta \mathbf{n} \cdot (2\mu\mathbf{E}) \cdot \mathbf{t}$	$(\mathbf{V} - \mathbf{v}_f) \cdot \mathbf{t} = \beta \mathbf{n} \cdot (2\mu\mathbf{E}) \cdot \mathbf{t}$
Interphasic velocity jump	$0 = -\beta \mathbf{n} \cdot (2\mu_e \mathbf{e}_f) \cdot \mathbf{t}$	$(\mathbf{v}_s - \mathbf{v}_f) \cdot \mathbf{t} = -\beta \mathbf{n} \cdot \sigma_s \cdot \mathbf{t}$

in the limit of $\phi_f \rightarrow 0$. For BC2, the interfacial permeability η drops out, and we need only require $\beta \rightarrow 0$. Thus the interphasic velocity jump vanishes: $\mathbf{v}_s - \mathbf{v}_f \rightarrow 0$, and we recover the usual no-slip boundary condition from the tangential velocity jump. The no-penetration condition is automatically satisfied for BC2 by the traction balance.

In the opposite limit of $\phi_f \rightarrow 1$, the boundary conditions reduce to those in Table III, with a certain symmetry to Table II. For BC1, the requirement of $\beta \rightarrow 0$ recovers the continuity of normal and tangential velocities across the ‘‘interface’’ as the gel particle approaches a fluid drop and the interface disappears. For BC2, $\beta \rightarrow 0$ and $\eta \rightarrow 0$ will ensure velocity continuity across the ‘‘interface.’’ Note that the limit of σ_s is ambiguous in this case, but does not affect the above argument.

To summarize, the two sets of boundary conditions will reach physically reasonable limits if the interfacial slip and permeability coefficients obey the following:

- (1) BC1: $\beta \rightarrow 0$ and $\eta \rightarrow 0$ as $\phi_f \rightarrow 0$; $\beta \rightarrow 0$ as $\phi_f \rightarrow 1$,
- (2) BC2: $\beta \rightarrow 0$ and $\eta \rightarrow 0$ as $\phi_f \rightarrow 1$; $\beta \rightarrow 0$ as $\phi_f \rightarrow 0$.

Experimental data will be required if one wishes to model the functional dependence of $\beta(\phi_f)$ and $\eta(\phi_f)$.

V. CONCLUDING REMARKS

We have adapted the energy dissipation principle of Young *et al.* [21] to derive an alternative set of boundary conditions (BCs) between a hydrogel and a surrounding solvent. The two sets of boundary conditions, BC1 of Young *et al.* [21] and BC2 of the present work, appear similar in postulating various velocity jumps at the interface that depend linearly on the stresses on either side of the interface or their imbalance. However, they predict distinct flow patterns in a simple 1D shear flow of the solvent over a gel layer described by the poroelastic Brinkman flow. Whereas BC1 predicts no entrained flow inside the gel, the BC2 predicts a shear flow profile. The latter is comparable to predictions of the earlier model of Minale [19] but differs in important aspects.

 TABLE III. The two sets of boundary conditions in the limit of $\phi_f \rightarrow 1$.

Physical meaning	BC1	BC2
Kinematics	$\mathbf{n} \cdot \mathbf{v}_s = v_\Gamma$	
Fluid continuity	$\mathbf{n} \cdot (\mathbf{V} - \mathbf{v}_f) = 0$	
Total traction balance	$\mathbf{n} \cdot (2\mu\mathbf{E} - P\mathbf{I}) = \mathbf{n} \cdot (2\mu_e \mathbf{e}_f - p\mathbf{I})$	
Normal velocity jump	$(\mathbf{V} - \mathbf{v}_s) \cdot \mathbf{n} = 0$	$(\mathbf{V} - \mathbf{v}_f) \cdot \mathbf{n} = \eta \mathbf{n} \cdot (2\mu_e \mathbf{e}_f - \sigma_s) \cdot \mathbf{n}$
Tangential velocity jump	$(\mathbf{V} - \mathbf{v}_s) \cdot \mathbf{t} = \beta \mathbf{n} \cdot (2\mu\mathbf{E}) \cdot \mathbf{t}$	$(\mathbf{V} - \mathbf{v}_f) \cdot \mathbf{t} = \beta \mathbf{n} \cdot (2\mu\mathbf{E}) \cdot \mathbf{t}$
Interphasic velocity jump	$(\mathbf{v}_f - \mathbf{v}_s) \cdot \mathbf{t} = -\beta \mathbf{n} \cdot (2\mu_e \mathbf{e}_f) \cdot \mathbf{t}$	$0 = -\beta \mathbf{n} \cdot \sigma_s \cdot \mathbf{t}$

For both BC1 and BC2, we have explored their limiting forms when the Brinkman medium tends to the Darcy limit and when the gel approaches the one-phase limits of impermeable solid and pure fluid. For steady flows in the Darcy limit, BC1 and BC2 are essentially identical to each other. In the one-phase limits, the slip coefficient β and the interface permeability η should vanish in order to recover expected fluid-solid BCs or fluid-fluid continuity. This provides guides for modeling β and η as functions of the void fraction in the gel.

An open question is which of the three sets of BCs (BC1, BC2, and that of Minale [19]) more closely represents reality. Having compared their predictions in the simple 1D shear flow problem, we realize that steady flows in the Darcy limit will not be a sensitive test to discriminate between BC1 and BC2. Thus, the BCs should be tested in numerical computations of nontrivial and time-dependent Brinkman flows, with the results compared with measurements in carefully designed experiments. A promising experiment is the oscillatory shear flow of Hobbie *et al.* [12] of a liquid over a gel layer. Although the focus of their study is the microrheology of the gel, the time-dependent interfacial motion could serve as a test for our boundary conditions.

ACKNOWLEDGMENTS

This work was supported by NSF-DMS 1614863 and 1412789 (to Y.-N.Y.) and NSERC RGPIN-2019-04162 (to J.J.F.). The authors also acknowledge helpful discussions with Lex Li, Chun Liu, Arun Ramadranchan, and Pengtao Yue. Y.-N.Y. acknowledges support from Flatiron Institute, part of Simons Foundation.

-
- [1] W. J. Polacheck, R. Li, S. G. M. Uzel, and R. D. Kamm, Microfluidic platforms for mechanobiology, *Lab Chip* **13**, 2252 (2013).
 - [2] J. D. Carrico, T. Tyler, and K. K. Leang, A comprehensive review of select smart polymeric and gel actuators for soft mechatronics and robotics applications: Fundamentals, freeform fabrication, and motion control, *Int. J. Smart Nano Mater.* **8**, 144 (2017).
 - [3] R. Burridge and J. B. Keller, Poroelasticity equations derived from microstructures, *J. Acoust. Soc. Am.* **70**, 1140 (1981).
 - [4] J. M. Carcione, Biot theory for porous media, in *Wave Fields in Real Media*, 3rd ed. (Elsevier, Oxford, 2015), p. 299, Chap. 7.
 - [5] N. G. Cogan and J. P. Keener, The role of the biofilm matrix in structural development, *Math. Med. Biol.* **21**, 147 (2004).
 - [6] W. Strychalski, C. A. Copos, O. L. Lewis, and R. D. Guy, A poroelastic immersed boundary method with applications to cell biology, *J. Comp. Phys.* **282**, 77 (2015).
 - [7] W. Strychalski and R. D. Guy, Intracellular pressure dynamics in blebbing cells, *Biophys. J.* **110**, 1168 (2016).
 - [8] C. W. MacMinn, E. R. Dufresne, and J. S. Wettlaufer, Large Deformation of a Soft Porous Material, *Phys. Rev. Appl.* **5**, 044020 (2016).
 - [9] Y. Mori, H. Chen, C. Micek, and M.-C. Calderer, A dynamic model of polyelectrolyte gels, *SIAM J. Appl. Math.* **73**, 104 (2013).
 - [10] X. Zhang, L. Li, and C. Luo, Gel integration for microfluidic applications, *Lab Chip* **16**, 1757 (2016).
 - [11] H. Huang, Y. Yu, Y. Hu, X. He, O. Berk Usta, and M. L. Yarmush, Generation and manipulation of hydrogel microcapsules by droplet-based microfluidics for mammalian cell culture, *Lab Chip* **17**, 1913 (2017).
 - [12] E. K. Hobbie, S. Lin-Gibson, and S. Kumar, Non-Brownian Microrheology of a Fluid-Gel Interface, *Phys. Rev. Lett.* **100**, 076001 (2008).
 - [13] G. S. Beavers and D. D. Joseph, Boundary conditions at a naturally permeable wall, *J. Fluid Mech.* **30**, 197 (1967).

- [14] J. A. Ochoa-Tapia and S. Whitaker, Momentum transfer at the boundary between a porous medium and a homogeneous fluid—I. Theoretical development, *Int. J. Heat Mass Transfer* **38**, 2635 (1995).
- [15] J. A. Ochoa-Tapia and S. Whitaker, Momentum transfer at the boundary between a porous medium and a homogeneous fluid—II. Comparison with experiment, *Int. J. Heat Mass Transfer* **38**, 2647 (1995).
- [16] B. Alazmi and K. Vafai, Analysis of fluid flow and heat transfer interfacial conditions between a porous medium and a fluid layer, *Int. J. Heat Mass Transfer* **44**, 1735 (2001).
- [17] M. L. Bars and M. G. Worster, Interfacial conditions between a pure fluid and a porous medium: Implications for binary alloy solidification, *J. Fluid Mech.* **550**, 149 (2006).
- [18] M. Minale, Momentum transfer within a porous medium. I. Theoretical derivation of the momentum balance on the solid skeleton, *Phys. Fluids* **26**, 123101 (2014).
- [19] M. Minale, Momentum transfer within a porous medium. II. Stress boundary condition, *Phys. Fluids* **26**, 123102 (2014).
- [20] M. Minale, Modelling the flow of a second order fluid through and over a porous medium using the volume averages. II. The stress boundary condition, *Phys. Fluids* **28**, 023103 (2016).
- [21] Y.-N. Young, Y. Mori, and M. J. Miksis, Slightly deformable Darcy drop in linear flows, *Phys. Rev. Fluids* **4**, 063601 (2019).
- [22] K. Vafai and S. J. Kim, Fluid mechanics of the interface region between a porous medium and a fluid layer—An exact solution, *Int. J. Heat Mass Transfer* **11**, 254 (1990).
- [23] S. Whitaker, Flow in porous media. I: A theoretical derivation of Darcy's law, *Transp. Porous Med.* **1**, 3 (1986).
- [24] S. S. Antman, in *Nonlinear Problems of Elasticity* (Springer, New York, 1995), p. 478.
- [25] P. Angot, B. Goyeau, and J. A. Ochoa-Tapia, Asymptotic modeling of transport phenomena at the interface between a fluid and a porous layer: Jump conditions, *Phys. Rev. E* **95**, 063302 (2017).
- [26] N. Nishiyama and T. Yokoyama, Permeability of porous media: Role of the critical pore size, *J. Geophys. Res. Solid Earth* **122**, 6955 (2017).
- [27] S. K. Lai, Y. Y. Wang, K. Hida, R. Cone, and J. Hanes, Nanoparticles reveal that human cervicovaginal mucus is riddled with pores larger than viruses, *Proc. Natl. Acad. Sci. USA* **107**, 598 (2010).
- [28] J. Kirch, A. Schneider, B. Abou, A. Hopf, U. F. Schaefer, M. Schneider, C. Schall, C. Wagner, and C. M. Lehr, Optical tweezers reveal relationship between microstructure and nanoparticle penetration of pulmonary mucus, *Proc. Natl. Acad. Sci. USA* **109**, 18355 (2012).
- [29] Y. Y. Wang, S. K. Lai, L. M. Ensign, W. Zhong, R. Cone, and J. Hanes, The microstructure and bulk rheology of human cervicovaginal mucus are remarkably resistant to changes in pH, *Biomacromolecules* **14**, 4429 (2013).
- [30] J. P. Pearson, P. I. Chater, and M. D. Wilcox, The properties of the mucus barrier, a unique gel—How can nanoparticles cross it? *Ther. Deliv.* **7**, 229 (2016).
- [31] N. Annabi, J. W. Nichol, X. Zhong, C. Ji, S. Koshy, A. Khademhosseini, and F. Dehghani, Controlling the porosity and microarchitecture of hydrogels for tissue engineering, *Tissue Eng. Part B* **16**, 371 (2010).
- [32] L. Zhao, X. Li, J. Zhao, S. Ma, X. Ma, D. Fan, C. Zhu, and Y. Liu, A novel smart injectable hydrogel prepared by microbial transglutaminase and human-like collagen: Its characterization and biocompatibility, *Mater. Sci. Eng. C* **68**, 317 (2016).
- [33] X. Song, C. Zhu, D. Fan, Y. Mi, X. Li, R. Z. Fu, Z. Duan, Y. Wang, and R. R. Feng, A novel human-like collagen hydrogel scaffold with porous structure and sponge-like properties, *Polymers* **9**, 638 (2017).
- [34] C. Cottin-Bizonne, A. Steinberger, B. Cross, O. Raccurt, and E. Charlaix, Nanohydrodynamics: The intrinsic flow boundary condition on smooth surfaces, *Langmuir* **24**, 1165 (2008).
- [35] P. A. Martin, Two-dimensional Brinkman flows and their relation to analogous Stokes flows, *IMA J. Appl. Math.* **84**, 912 (2019).